Theor Chim Acta (1992) 82: 285–298

Theoretica Chimica Acta

Investigation of electron distribution and hyperfine properties of hemin by first-principles Hartree–Fock self-consistent field procedure

N. Sahoo, K. Ramani Lata, and T. P. Das
Department of Physics, State University of New York at Albany, Albany, New York 12222, USA

Received December 12, 1990/Accepted October 4, 1991

Summary. As part of a program for first-principles quantitative study of hyperfine properties of large biological molecules, we have applied the Self-Consistent Field Unrestricted Hartree–Fock procedure to investigate the electronic structure of hemin, the associated charge and unpaired spin population distributions and the hyperfine constants of ^{57}Fe, ^{14}N, ^{13}C, ^{1}H and ^{35}Cl nuclei. The results of the present work indicate significantly more localized charge and spin distributions than were found earlier by the semi-empirical Self-Consistent Charge Extended Hückel procedure. The theoretical values of the ^{57}Fe, ^{14}N and methene proton hyperfine constants, the only nuclei for which experimental data are available, are found to be -34.99, 11.89 and -1.50 MHz in satisfactory agreement with the experimental values of -26.47, 7.55 and -1.014 MHz, respectively. The contact and dipolar contributions to the hyperfine constants and their breakdowns into direct and exchange polarization contributions are analyzed. Possible sources that could bridge the remaining gap between experiment and theory will be analyzed.

Key words: Hemin – Hyperfine properties – First-principles UHF

1 Introduction

With the advent of sophisticated Gaussian codes [1] to investigate electronic structures of molecular systems it has now become possible to study electronic distributions over large molecules and associated hyperfine properties by the first-principles Unrestricted Hartree–Fock (UHF) procedure [2]. Applications have already been made to a number of large molecular systems [3] including clusters [4–6] that simulate infinite size solid state systems. This is therefore an opportune time to carry out UHF investigations of hyperfine properties in heme systems and hemoglobin derivatives to compare with experimental results by magnetic resonance [7–10] and Mössbauer [11] techniques.

The electronic structures of heme systems and hemoglobin derivatives have been investigated earlier [12–16], primarily by approximate methods and in a few cases [17] by the Hartree–Fock procedure. The hyperfine properties of these systems, which provide very useful insights into the nature of their electron

distributions, have been studied [13–16] mainly by approximate procedures, most extensively [14–16, 18–21] by the semi-empirical Self-Consistent Charge Extended Hückel (SCCEH) procedure [12, 16, 22]. More recently, the Coulomb Corrected Self-Consistent Charge Extended Hückel (CCSCCEH) procedure [23, 24], which involves modifications to the SCCEH procedure to take account of the Coulomb interaction between the electrons primarily associated with a particular atom and charges on other atoms, has also been utilized in a few systems.

The aim of our work is not only to obtain a first-principles understanding of specific systems but also to assess the capability of current approaches to the Hartree–Fock procedure for a variety of large biological systems. The system hemin was chosen because there are extensive hyperfine data available [25] for it and also because it has been studied earlier by SCCEH [26] and CCSCCEH [24] procedures. To the best of our knowledge, this is the first extensive investigation of the hyperfine properties of a heme compound by the first-principles UHF procedure.

Section 2 will present briefly the procedure utilized, Sect. 3 the results and their discussion, and Sect. 4 the conclusions from the present work and possible directions for improvements in the future.

2 Procedure

The arrangement of atoms for the model of hemin molecule used in our work is presented in Fig. 1. The overall geometry for the molecule was assumed to be tetragonal as in earlier work using the SCCEH [26] and CCSCCEH [24] procedures. The Fe atom was assumed to be located 0.455 Å above the center of the porphyrin ring in keeping with earlier investigations [15, 26] by approximate procedures, for making comparisons of the calculated hyperfine and other properties, although the available X-ray data [27] suggest a slightly different value, 0.475 Å. The Cl atom was also moved by 0.02 Å when the Fe atom was moved to 0.455 Å above the porphyrin center, to keep the Fe–Cl distance the same as from the X-ray data [27], locating the Cl at a height of 2.67 Å above the

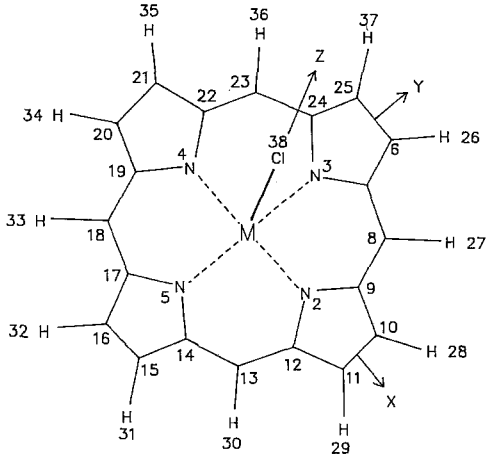

Fig. 1. Molecular structure of iron porphyrin chloride – model system used for hemin

center of the porphyrin plane instead of 2.69 Å from the X-ray data. This adjustment keeps the Fe–Cl interaction unchanged and since the Fe–N distances are also virtually unchanged by moving the Fe atom perpendicular to the porphyrin plane by 0.02 Å, the electronic structure is expected to be unaffected by this adjustment. As will be discussed in Sect. 3, this was indeed found to be the case. To keep the calculation within practicable limits, the side-chains in the protoporphyrin system were replaced by hydrogen atoms, which still involved 203 electrons. Experimental data on hyperfine properties are available for the nuclei of iron, nitrogen, methene carbon and methene hydrogen which will be compared with our theoretical results. One does not expect the electron distributions on these atoms, which are a number of bond-lengths away from the pyrrole carbons, to be influenced significantly by the replacement of the side-chains at the latter by hydrogens.

The UHF procedure [2] used in the present work, employed the Gaussian 88 code. The following basis set [28] was used, namely, for iron [29], 12*s*, 6*p* and 5*d* primitive Gaussian functions contracted to 8*s*(4, 2, 1, 1, 1, 1), 4*p*(3, 1, 1, 1) and 3*d*(3, 1, 1), for carbon and nitrogen atoms [30], 8*s* and 4*p* primitive Gaussians contracted to 2*s*(6, 2) and 1*p*(4), for hydrogen [30], 4*s* Gaussians contracted to 2*s*(3, 1) and for chlorine [31], 12*s* and 8*p* Gaussians contracted to 4*s*(6, 2, 2, 2) and 2*p*(6, 2). The total number of basis functions with this choice added up to 177 for hemin and the total number of electrons to 203, with 104 in up spin (α) and 99 in down spin (β) states. This choice of functions is expected to be appropriate for study of hyperfine properties from our recent work with paramagnetic aquoions [28] and a number of molecular and solid-state systems [32].

The charges and unpaired spin populations on the atoms were obtained through Mulliken population analysis [33] using the UHF electronic wavefunctions for the system. They provide valuable insights respectively about the extent of covalent bonding between the atoms and the expected natures of the magnetic and hyperfine properties of the system. In the SCCEH and CCSCCEH procedures [24, 26] where the paired orbitals are not spin-polarized, the spin populations on the atoms arise from only the unpaired spin electrons, and are always positive. However with the UHF procedure, where spin-polarization effects are included, the unpaired spin populations on some atoms could be negative, indicating larger down spin populations than up. We shall see evidence for this for some of the atoms distant from the iron atom.

Turning next to the hyperfine interactions associated with the various nuclei in the molecule, the expression for the contact hyperfine interaction constant $A_C(\vec{R}_N)$ in MHz for a nucleus with position vector $\vec{R}_N$ with respect to the chosen origin is given by [28, 34]:

$$A(\vec{R}_N) = \frac{2 \times 10^{-6}}{3S} \gamma_e \gamma_N \hbar a_0^{-3} \left[\sum_{\nu} \{ |\psi_{\nu\uparrow}(\vec{R}_N)|^2 - |\psi_{\nu\downarrow}(\vec{R}_N)|^2 \} + \sum_{\mu} |\psi_{\mu\uparrow}(\vec{R}_N)|^2 \right] \quad (1)$$

while the expressions for the components of the dipolar hyperfine tensor are given by:

$$B_{ij}(\vec{R}_N) = \frac{10^{-6} \gamma_e \gamma_N \hbar a_0^{-3}}{4\pi S} \left[\sum_{\nu} \{ \langle \psi_{\nu\uparrow} | O_{ij} | \psi_{\nu\uparrow} \rangle - \langle \psi_{\nu\downarrow} | O_{ij} | \psi_{\nu\downarrow} \rangle \} + \sum_{\mu} \langle \psi_{\mu\uparrow} | O_{ij} | \psi_{\mu\uparrow} \rangle \right] \quad (2)$$

where:

$$O_{ij} = \left(\frac{3 r_{Ni} r_{Nj} - r_N^2 \delta_{ij}}{r_N^5} \right) \quad (3)$$

In Eqs. (1) and (2), r_{Ni} and r_{Nj} refer to the components of the position vector $\vec{r}_N$ of an electron with respect to the nucleus, $\psi_{\mu\uparrow}$ and $\psi_{\nu\downarrow}$ refer to the molecular orbitals for the states μ with spin up and states ν with spin down respectively, the summation over μ referring to the unpaired spin states and over ν to the paired including the core states. The γ_N and γ_e refer to the nuclear and electronic gyromagnetic ratios and S to the total electronic spin.

The terms in the first summation in each of Eqs. (1) and (2) representing the exchange polarization [ECP] contributions were calculated directly here unlike in earlier work [24, 26] involving the SCCEH and CCSCCEH procedures $\psi_{\nu\uparrow}$ and $\psi_{\nu\downarrow}$ were assumed equal, the ECP effect being estimated there for ^{57}Fe and neglected for ^{14}N and protons.

Once the components $B_{ij}(\vec{R}_N)$ are obtained one can diagonalize the tensor $\vec{\vec{B}}(\vec{R}_N)$ to determine its principal components. However, often in experimental measurements, depending on the technique, one can obtain specific combinations of A and B, for instance [35]: $(A + B_{zz})$ or [11] $(A + B_{xx})$.

3 Results and discussion

Considering first the charges on the various atoms listed in Table 1, one notices two main features from these results. The first is that as compared to the SCCEH results [26], the CCSCCEH results [24] for the charges are in general closer to the present UHF results. An exception is the methene hydrogen, for which the charge from the CCSCCEH procedure is closer to the SCCEH result, both being significantly smaller than the UHF value. Secondly, the UHF results indicate greater charge separations than in both the SCCEH and CCSCCEH cases indicating lesser covalent bonding than was found earlier by the latter approximate procedures. However, the departure of the UHF charges from a fully ionic model, such as +2.05 for iron as compared to +3 and −0.518 for chlorine as compared to −1, suggest that there is still significant covalent bonding between iron and its neighbors.

The unpaired spin populations on the various atoms are presented in the second half of Table 1. In contrast to the case of the charges, no results are presented for the CCSCCEH procedure, for which no published results are

Table 1. Effective charges and unpaired spin populations on atoms in hemin

Atom	Charge			Unpaired spin population[c]	
	SCCEH[a]	CCSCCEH[b]	This work	SCCEH[a]	This work
Fe_1	0.251	1.260	2.045	3.240	4.527
N_3	−0.176	−0.578	−0.461	0.245	0.091
C_6	−0.043	—	−0.206	0.017	0.002
C_7	0.033	—	0.055	0.014	−0.034
C_8	−0.016	—	−0.210	0.034	0.038
H_{26}	0.062	—	0.193	0.000	−0.003
H_{27}	0.088	0.050	0.206	0.001	0.000
Cl_{38}	−0.244	—	−0.518	0.388	0.227

[a] Ref. [26]
[b] Ref. [24]
[c] Unpaired spin populations by the CCSCCEH procedure are not available in the literature

available. However, the closeness of the calculated hyperfine constants by the SCCEH [26] and CCSCCEH [24] procedures suggests that the unpaired spin populations for the two cases are close to each other. The spin populations from the UHF procedure are seen from Table 1 to indicate much greater spin-localization than those from the SCCEH procedure. However, the spin population on the iron atom by the present UHF investigation is 4.527, which is about 90 percent of the value of 5.0 that one would have expected for complete localization. Thus there is still significant migration of spin population from iron to the nitrogens and other atoms of the porphyrin substrate. Additionally, the importance of the exchange polarization effect inherent in the UHF procedure is visible from the negative spin populations on the pyrrole carbon C_7 and hydrogen H_{26}. The corresponding populations are positive for the SCCEH procedure in which exchange polarization effects are not included.

Turning next to the hyperfine interaction, the calculated isotropic contact parameters A and the dipolar components B_{ij} for the ^{57}Fe, ^{35}Cl, ^{14}N, ^{13}C and ^{1}H nuclei are listed in Table 2. As mentioned in Sect. 2, the side-chains in the protoporphyrin substrate have been replaced by hydrogens in Fig. 1. Further, in view of the fact that crystal structure data indicate very little departure from tetragonal symmetry and the use of the latter considerably reduces computational effort, we have assumed tetragonal symmetry. The small departure from this needs to be considered [35] only if one is interested in interpreting the very small observed differences among, for instance, the ^{14}N nuclei in fluoromyglobin [36]. In view of the tetragonal symmetry, a number of nuclei in the system are equivalent and only one member of each group is listed in Table 2.

Table 2 presents the calculated contact parameters and dipolar tensor components in the coordinate system shown in Fig. 1. By Mössbauer effect measurements [37] for the ^{57}Fe and ENDOR measurements [38] for the ^{14}N and ^{1}H nuclei, the techniques used so far for hyperfine interaction measurements on these nuclei, one obtains experimental values of $(A + B_{xx})$ and $(A + B_{zz})$, respectively, with the axes as in Fig. 1. If the principal components of the dipolar hyperfine tensor are needed, they can be obtained from the components in Table 2 through appropriate diagonalization.

To check the sensitiveness of the results obtained for the properties in Tables 1 and 2 with respect to the position of the Fe atom, the calculation was repeated with the Fe atom at 0.475 Å, and the Cl atom at 2.69 Å, above the porphyrin center, as given by the X-ray data [27]. The total energy was virtually unchanged up to the seventh significant figure as compared to that for the Fe and Cl atoms at 0.455 Å and 2.67 Å above the porphyrin center. The charges and unpaired spin populations on the atoms were the same up to the fourth and third significant figures, respectively. The hyperfine properties were within 0.2% for ^{57}Fe and ^{14}N and less than 4% different for ^{35}Cl and ^{1}H. The results in Tables 1–3 are therefore closely representative of those for the actual crystal structure.

From Table 2, the contact term for ^{57}Fe is seen to be negative as is the case in most iron compounds [39] and iron metal [40]. It is two orders of magnitude larger than the dipolar components, the latter being axially symmetric because of the tetragonal symmetry assumed for the heme unit. The calculated hyperfine constant $(A + B_{xx})$ parallel to the heme plane is -35.25 MHz, corresponding to a hyperfine field of -639.29 kG. The corresponding experimental values from Mössbauer measurements are -26.47 MHz and -480 kG [35] with the same sign as theory and about 25 percent smaller in magnitude.

Table 2. Hyperfine interaction parameters (MHz) for various nuclei in hemin

Nucleus	Contact parameter A	Dipolar parameters B_{xx}	B_{yy}	B_{zz}	B_{xy}	B_{yz}	B_{zx}	Net[a] hyperfine constant	expt
$^{57}Fe_1$	−35.514	0.264	0.264	−0.527	0.000	0.000	0.000	−35.251	−26.47[b]
$^{14}N_3$	12.128	−1.221	1.457	−0.236	0.000	−0.449	0.000	11.892	7.55 ± 0.05[c]
$^{13}C_6$	1.148	0.567	−0.214	−0.353	−0.088	−0.015	0.075	0.795	—
$^{13}C_7$	−3.682	1.344	0.051	−1.395	−0.745	−0.101	0.264	−5.077	—
$^{13}C_8$	3.804	−0.190	−0.190	0.380	−0.671	−0.140	0.140	4.184	—
$^{1}H_{26}$	0.057	−0.413	0.943	−0.530	0.371	−0.139	−0.037	−0.473	—
$^{1}H_{27}$	−0.668	0.419	0.419	−0.837	1.486	−0.183	−0.183	−1.505	1.014 ± 0.003[d]
$^{35}Cl_{38}$	4.061	−3.140	−3.140	6.281	0.000	0.000	0.000	10.342	—

[a] For the ^{57}Fe nucleus, the net hyperfine constant refers to a direction parallel to the heme plane and is given by $(A + B_{xx})$. For the rest of the nuclei, the net hyperfine constant refers to a direction perpendicular to the heme plane and is given by $(A + B_{zz})$. The hyperfine constant for ^{57}Fe can be converted to the hyperfine field in kilogauss using the fact that 1 MHz = 18.136 KG.

[b] Ref. [35] The experimental result of 480 KG for the hyperfine field has been converted to MHz for the hyperfine constant

[c] Ref. [38]

[d] Ref. [41]

For the ^{14}N hyperfine interaction the contact term, unlike for ^{57}Fe is seen from Table 2 to be positive, being dominated by the direct term in Eq. (1). It is again larger than the dipolar components but by only one order of magnitude instead of two. Additionally, as one can notice from the component B_{yz} in Table 2 the dipolar tensor is no longer axially symmetric. This is expected from the nature of the geometry around the ^{14}N nucleus. The appropriate quantity to compare with in this case, obtained from ENDOR measurements [38] is $(A + B_{zz})$, for which the theoretical value is seen from Table 2 to be 11.89 MHz, about 35 percent higher than the experimental value of 7.55 MHz, in somewhat lesser agreement than was the case for ^{57}Fe.

The one other nucleus for which the hyperfine constant is available [41] from ENDOR measurements, is H_{27}, corresponding to the methene protons. In this case, in contrast to the cases of ^{57}Fe and ^{14}N, the contact and dipolar interactions are of comparable magnitude. The progressive trend in this feature in going from ^{57}Fe to ^{14}N to $^{1}H_{27}$ is the result of the increasing distance between the center of the unpaired spin distribution, namely the iron atom, and the nucleus in question which reduces the s-type spin density at the latter arising from both direct and exchange polarization mechanisms. The dipolar contributions, being more long range in character, have significant contribution from the unpaired spin population on iron, in addition to local contributions from orbitals on the atom in question. The theoretical value of $(A + B_{zz})$ is found to be -1.50 MHz, about 33 percent larger than the experimentally obtained magnitude of (1.014 ± 0.003) MHz.

For the rest of the nuclei listed in Table 2, ^{35}Cl, three species of ^{13}C and $^{1}H_{26}$, no experimental hyperfine data are presently available. It will be helpful to have such data available in the future to compare with the theoretical results in Table 2. For the proton corresponding to H_{26} it would be necessary to make measurements with a porphyrin substrate, where the side-chains are absent, instead of protoporphyrin [38]. The contact contribution for $^{1}H_{26}$ is comparable in order of magnitude to the dipolar while for the ^{13}C nuclei, the trend is intermediate between ^{14}N and $^{1}H_{27}$, these features being understandable by the arguments in the preceding paragraph. For ^{35}Cl, the contact and dipolar contributions are also comparable, but the reasoning is now different. The contact contribution arises primarily from the diffuse $4s$ iron orbital character in the unpaired spin orbitals as compared to the dipolar which arises from the more compact $3p$, the two contributions being still comparable because of the larger multiplying factor in Eq. (1) as compared to Eq. (2).

Table 3 lists the relative contributions from the paired and unpaired spin orbitals to the contact and dipolar components of the hyperfine interactions for all the nuclei. These provide insights into the relative importance of direct and exchange polarization effects which were not available before when the latter effects were estimated [24, 26] in contrast to the quantitative results available with the UHF procedure used here. For this reason, and because they are helpful in assessing the possible sources that could bridge the differences between experiment and theory in Table 2, we shall briefly discuss the nature of the direct and exchange polarization contributions for the ^{57}Fe and ^{14}N nuclei and methene protons.

Considering first the contact contribution, in the case of ^{57}Fe, the direct contribution is seen from Table 3 to be small and positive which is strongly dominated by the negative contribution from the paired spin orbitals. This is expected since as in ionic iron compounds [39] like Fe_2O_3, the unpaired spin

Table 3. Contributions from unpaired and paired states to the hyperfine interaction parameters (MHz) for various nuclei in hemin

Nucleus	Nature of contribution	Contact parameter A	Dipolar parameters B_{xx}	B_{yy}	B_{zz}	B_{xy}	B_{yz}	B_{zx}
	Unpaired	1.225	1.013	1.013	−2.025	0.0	0.0	0.0
$^{57}Fe_1$	Paired	−36.738	−0.749	−0.749	1.498	0.0	0.0	0.0
	Total	−35.514	0.264	0.264	−0.527	0.0	0.0	0.0
	Unpaired	0.608	−0.597	1.246	−0.649	0.0	−0.417	0.0
$^{14}N_3$	Paired	11.520	−0.625	0.212	0.413	0.0	−0.032	0.0
	Total	12.128	−1.221	1.457	−0.236	0.0	−0.449	0.0
	Unpaired	13.039	0.438	−0.098	−0.341	−0.018	−0.012	0.075
$^{13}C_6$	Paired	−11.891	0.129	−0.117	−0.012	−0.069	−0.003	−0.001
	Total	1.148	0.567	−0.214	−0.353	−0.088	−0.015	0.075
	Unpaired	9.571	0.932	−0.190	−0.742	−0.653	−0.076	0.257
$^{13}C_7$	Paired	−13.252	0.412	0.241	−0.653	−0.092	−0.025	0.007
	Total	−3.682	1.344	0.051	−1.395	−0.745	−0.101	0.264
	Unpaired	9.995	0.257	0.257	−0.513	−0.508	−0.123	0.123
$^{13}C_8$	Paired	−6.192	−0.447	−0.447	0.894	−0.163	−0.017	0.017
	Total	3.804	−0.190	−0.190	0.380	−0.671	−0.140	0.140
	Unpaired	0.363	−0.270	0.949	−0.679	0.548	−0.135	−0.035
$^{1}H_{26}$	Paired	−0.306	−0.143	−0.007	0.149	−0.178	−0.004	−0.002
	Total	0.057	−0.413	0.943	−0.530	0.371	−0.139	−0.037
	Unpaired	0.341	0.465	0.465	−0.930	1.247	−0.175	−0.175
$^{1}H_{27}$	Paired	−1.009	−0.046	−0.047	0.093	0.239	−0.008	−0.008
	Total	−0.668	0.419	0.419	−0.837	1.486	−0.183	−0.183
	Unpaired	225.474	−0.571	−0.571	1.142	0.0	0.0	0.0
$^{35}Cl_{38}$	Paired	−221.413	−2.569	−2.569	5.138	0.0	0.0	0.0
	Total	4.061	−3.140	−3.140	6.281	0.0	0.0	0.0

valence orbital is composed primarily of iron $3d$ character with small admixtures of p and s orbitals, the small positive contribution arising from the latter and the tails of the admixed nitrogen orbitals. The negative exchange polarization contribution results from the dominant $2s$ contribution, a feature similar to that in free iron atom [42], iron metal [40], Fe^{+3} ion [43] and ionic compounds [39].

For the ^{14}N nucleus, from Table 3, the exchange polarization contribution is again seen to be the dominant one but is now positive with the same sign as the direct effect. This feature is understandable from a consideration of the situation in the free atom [44] where the valence electrons have purely $2p$ character with zero direct contribution, the hyperfine interaction resulting from the stronger positive exchange polarization contribution from the $2s$ core orbitals as compared to the negative contribution from the $1s$ core orbitals. In hemin, the unpaired spin orbitals have primarily iron $3d$ character with some admixtures of nitrogen $2p$ and $2s$ characters, the latter component leading to the small direct contribution to the ^{14}N hyperfine constant. The paired spin molecular orbitals leading to the exchange polarization contribution are composed primarily of nitrogen $2s$ and $2p$ orbitals which are exchange polarized by the unpaired spin orbitals, primarily the nitrogen $2s$ and $2p$ components. The admixture of $2p$ character to the paired spin molecular orbitals with primarily $2s$ character, which make the major contribution to the exchange polarization effect, makes their exchange interaction with the $2p$ components of the unpaired spin orbitals substantially stronger than the corresponding interaction between the valence $2p$ orbitals and core $2s$ orbitals in the atom. This leads to a greater dominance of the positive exchange polarization contribution from the paired spin $2s$ type molecular orbitals over the negative contribution from the nitrogen core $1s$ orbitals than was the case in the free atom [44]. This appears to be the major reason for the sizeable positive exchange polarization effect for the ^{14}N hyperfine interaction in Table 3.

For the methene proton, the exchange polarization and direct contributions are seen from Table 3 to be of comparable order of magnitude in contrast to the situations for ^{57}Fe and ^{14}N nuclei. The negative exchange polarization contribution is expected to be the result of the exchange interaction between unpaired spin orbitals with π-character on the adjacent methene carbon and the paired spin orbitals of the CH bond (involving primarily hydrogen $1s$ character at the H-site) as is the usual feature in aromatic compounds [45]. The weaker exchange polarization contribution relative to direct as compared to ^{57}Fe and ^{14}N nuclei is more complicated to understand, but is probably a result of the fact that the exchange polarization effect for the latter for which the corresponding atoms have core electrons, is a result of mainly one-center exchange interactions while for the methene proton, the exchange effect is primarily two-center in nature [45].

As regards the ^{13}C and ^{35}Cl hyperfine interactions listed in Table 3, for which experimental data are currently unavailable, for the ^{13}C nuclei, the mechanisms for the direct and exchange polarization effects are similar to those for the ^{14}N nuclei. The stronger direct contribution relative to the exchange polarization effect in Table 3 as compared to ^{14}N, is probably a result of the stronger hybridization of $2s$ and $2p$ orbitals in carbon, since they are closer energy than in the case of nitrogen. For ^{35}Cl, where the direct and exchange polarization effects are comparable in magnitude and opposite in sign, the reasons for this feature are expected to be more complex to understand as compared to those for the other nuclei.

As regards the dipolar effects, the direct and exchange contributions for ^{57}Fe are seen from Table 3 to be comparable in magnitude and opposite in sign leading to a small net positive contribution, which from Table 2 is very small compared to the contact effect. For the ^{14}N nuclei, the direct and exchange contributions can be seen from Table 3 to have the same sign and comparable magnitude but are both small compared to the contact effect. For the ^{13}C, which like ^{14}N are on the pyrrole rings, the direct and exchange contributions are again comparable and have the same sign while for the methene ^{13}C nuclei the two have opposite signs, making the net contribution significantly weaker than for the pyrrole carbons. The understanding of these features is more difficult than in the contact case, because one now has to consider the anisotropy of the spin density rather than the isotropic component which means that one has to pay more attention to p and d characters on the corresponding atoms.

For both the pyrrole and methene protons, particularly for the latter, the direct contribution is seen from Table 3 to be the dominant one, although the exchange polarization contribution is significant in size and opposite in sign. It is interesting to compare the net calculated contribution to the dipolar contribution with that from the often used [46–49] point dipole model where the entire magnetic moment of 5.0 Bohr magnetons associated with spin 5/2 is assumed to be localized at the iron site. Such comparisons have been attempted in the past but were handicapped by the lack of availability of quantitative results for the exchange polarization contributions which had only been estimated [24, 26] using semi-empirical formulas. Thus, using the point dipole model and employing the Fe-methene proton distance of 4.56 Å, the calculated dipolar hyperfine component B_{zz} comes out as -0.803 MHz, which appears to be in excellent agreement with the net calculated value of -0.837 MHz from Table 3. This close agreement is however seen to be somewhat fortuitous because the net value is seen from Table 3 to be composed of a number of contributions, 0.093 MHz from exchange polarization effect and -0.930 MHz from the direct effect, of which -0.727 MHz arises from the magnetic moment of 4.527 Bohr magnetons (Table 1) from the actual unpaired spin population on the Fe atom and the balance of -0.203 MHz from the magnetic moments on the other atoms. In view of this, one cannot assume the point dipole model to be generally valid in all heme compounds.

In looking for possible sources for further improvement in the agreement between theoretical hyperfine interaction constants and experiment, the results tabulated in Tables 2 and 3 and the preceding discussions regarding the relative contributions from contact and dipolar effects and direct and exchange polarization effects are very helpful. Thus for ^{57}Fe and ^{14}N nuclei, the contact contribution is the most important one and also in both these cases, the exchange polarization effect makes the dominant contribution to the contact contribution. For the methene proton, both the contact and dipolar contributions are comparable and the exchange and direct effects respectively make the major contributions in the two cases. The experimental results are in all three cases about thirty percent smaller in magnitude than theory. In order to improve agreement with experiment, one thus primarily needs a reduction in the exchange polarization contributions to the contact effects for the ^{57}Fe and ^{14}N hyperfine constants and in the same contribution or the direct dipolar contribution for the methene proton.

It is conceivable that these reductions could be brought about by the use of larger basis sets that could lead to more accurate Hartree–Fock molecular

wavefunctions than we have obtained. However, we have already used rather extensive basis sets (Sect. 2) that involve the limits of the computing facilities available to us. While one should examine the influence of more extensive basis sets in the future with advances in computational facilities, it does not seem likely that this is the main source of the limitation in accuracy.

The source we feel that should be explored in the future is the influence of many-body effects [43, 44]. Since we have used first-principles UHF theory, which is a strictly one-electron theory [50], there are no many-body effects included, in contrast to the cases where approximations to a strictly one-electron UHF theory are used and uncertain amounts of many-body effects may be present. One could therefore invoke the effects of many-body theory in a definitive sense in the present work. In view of the size and the large number of electrons involved in this molecule or related hemoglobin derivatives, many-body effects would be rather time-consuming to incorporate in a quantitative way for the hyperfine properties studied here which involve such an intimate knowledge of the electron distribution in so many different regions of the molecule. It would be very helpful to explore their importance through future investigation by the many-body perturbation theoretic procedure [43, 44, 51]. However, we shall try to draw some conclusions here regarding the type of improvements that many-body theory has to provide, from a comparison of the theoretical and experimental hyperfine constants in Tables 2 and 3.

Considering the ^{57}Fe nucleus first, a reduction in the theoretical hyperfine constant $(A + B_{xx})$ could be brought about primarily by a reduction in the exchange polarization contribution resulting from the exchange interaction of the unpaired spin valence electrons and the 2*s* core electrons of the iron. In view of the rather tight binding of the latter, making them less susceptible to perturbation by many-body effects, one should instead look for a delocalization of the unpaired spin molecular orbitals away from the ^{57}Fe nucleus. A similar examination of the ^{14}N hyperfine constant $(A + B_{zz})$ suggests that a reduction could occur by a delocalization away from the ^{14}N nucleus of both the unpaired and paired spin molecular orbitals. For the methene proton, since a major part of the direct dipolar contribution arises from the unpaired spin population on iron, it is not likely to be influenced significantly by changes in the electron distribution around the hydrogen atom. One thus has to look for a reduction in the exchange polarization contribution to the contact term. Such a reduction, as in the case of the ^{14}N nucleus, can come about through a delocalization of the paired and unpaired spin molecular orbitals away from the hydrogen atom.

In summary, the needed influence of many-body effects to improve agreement between theory and experiment [35, 38, 41] for the ^{57}Fe, ^{14}N and methene proton hyperfine interactions appears to be one of loosening or delocalization of the iron-like, nitrogen-like and hydrogen-like molecular orbitals from iron, nitrogen and hydrogen sites respectively. It will be interesting to see whether this trend is indeed found to occur, when one can carry out these difficult many-body calculations in the future.

4 Conclusion

The application of the first-principles Unrestricted Hartree–Fock procedure to the heme compound hemin, without any chosen parameters, as in semi-empirical methods, and without any approximation to the exchange interaction, leads to a

successful interpretation of the available hyperfine constants for the ^{57}Fe, ^{14}N and ^{1}H nuclei. The charge and unpaired spin population distributions come out as much more localized than was the case with the Self-Consistent Charge and Charge-Corrected Self-Consistent Charge procedures [26, 24]. In quantitative terms, the experimental hyperfine constants come out to be about thirty percent lower than the theoretical predictions. From an analysis of the contributions from direct and exchange polarization effects to the contact and dipolar mechanisms, it is suggested that many-body effects would have to lead to a loosening of the molecular orbitals to reduce their densities at the iron, nitrogen and hydrogen atoms below that one obtains from the present first-principles, strictly one-electron theory. It is also hoped that ^{13}C and ^{35}Cl hyperfine data will be available in the future in hemin to compare with our theoretical predictions and further assess the accuracy of the electron-distribution obtained by the present first-principles investigation.

Acknowledgements. This work was supported by a grant, CHE 8619660, from the Chemistry Division of the National Science Foundation. A major part of the computations was carried out at the Cornell National Supercomputer Facility, a resource of the Center for Theory and Simulation in Science and Engineering at Cornell University which receives major funding from the National Science Foundation and IBM Corporation and additional support from New York State and members of the Corporate Research Institute.

References

1. Frisch MJ, Head-Gordon M, Schlegel HB, Raghavachari K, Binkley JS, Gonzalez C, Defrees DJ, Fox DJ, Whiteside RA, Steeger R, Melius CF, Baker J, Martin R, Kahn LR, Stewart JJP, Fluder EM, Topiol S, Pople JA (1988) Gaussian 88. Gaussian Inc, Pittsburgh
2. Watson RE, Freeman AJ (1967) in: Freeman AJ, Frenkel RB (eds) Hyperfine interaction. Academic Press, NY; Pople JA, Nesbet RK (1959) J Chem Phys 22:571
3. Nordenskiold L, Laaksonen A, Kowalewski J (1982) J Am Chem Soc 104:379; Sahoo N, Das TP (1989) J Chem Phys 91:7740
4. Seel M, Bagus PS (1983) Phys Rev B28:2023 and references therein; Batra IP, Bagus PS, Herman K (1984) Phys Rev Lett 52:384; Malvido JC, Whitten JL (1982) Phys Rev B26:4458
5. Sahoo N, Mishra SK, Mishra KC, Coker A, Mitra CK, Snyder LC, Glodeanu A, Das TP (1983) Phys Rev Lett 60:913; Sahoo N, Sulaiman S, Mishra KC, Das TP (1989) Phys Rev B39:13389
6. Dev BN, Mohapatra SM, Sahoo N, Mishra KC, Gibson WM, Das TP (1988) Phys Rev B38:13335; Kelires PC, Das TP (1987) Hyperfine Interactions 34:285; Kelires PC, Mishra KC, Das TP (1987) Hyperfine Interactions 34:289
7. Scholes CP Isaacson RA, Feher G (1972) Biochem Biophys Acta 263:448; Feher G, Isaacson RA, Scholes CP, Nagel R (1973) Ann NY Acad Sci 206:86
8. Van Camp HL, Scholes CP, Mulks CF (1976) J Am Chem Soc 98:4094; Mulks CF, Scholes CP, Dickinson LC, Lapidot A (1979) J Am Chem Soc 101:1645; Peisach J (1975) Ann NY Acad Sci 244:187
9. Peisach J, Blumberg WE, Adler A (1973) Ann NY Acad Sci 206:310; Chien JCW (1969) J Chem Phys 51:4220; Doetschman DC, Utterback SG (1981) J Am Chem Soc 103:2847
10. LaMar GN, Overkamp M, Sick H, Gersonde K (1978) Biochemistry 17:352; Johnson ME, Fung LWM, Ho C (1977) J Am Chem Soc 99:1245; Shulman RG, Glarum SH, Karplus M (1971) J Mol Biol 57:93
11. Johnson CE (1966) Phys Lett 21:491; Lang G, Marshall W (1966) Proc Phys Soc London 87:3; Lang G (1970) Q Rev Biophys. 3, 1
12. Zerner M, Gouterman M, Kobayashi M (1966) Theor Chim Acta 6:363
13. Huynh BH, Case DA, Karplus M (1977) J Am Chem Soc 99:6103; Case DA, Huynh BH, Karplus M (1979) J Am Chem Soc 101:4433

14. Trautwein A, Zimmermann R, Harris FE (1975) Theor Chim Acta 37:89
15. Loew G, Kirchner RF (1975) J Am Chem Soc 97:7388; Loew G (1978) Biophys J 22:179
16. Han PS, Das TP, Rettig MF (1970) Theor Chim Acta 16, 1; Mallick MK, Chang JC, Das TP (1978) J Chem Phys 68:1462; Mishra SK, Roy JN, Mishra KC, Das TP (1989) Theor Chim Acta 75:195
17. Dedieu A, Rohmer MM, Veillard A (1976) in: Proc 9th Jerusalem Symp on Quantum Chem and Biochem, March 1976, B Pullman Ed, D. Reidel Publishing Company; Dedieu A, Rohmer MW, Bernard M, Veillard A (1976) J Am Chem Soc 98:3717
18. Rettig MF, Han PS, Das TP (1968) Theor Chim Acta 12:178 and (1969) 13:432; Han PS, Rettig MF, Ikenberry D, Das TP (1971) Theor Chim Acta 22:261; Chang JC, Ikenberry D, Das TP (1974) Theor Chim Acta 35:361 and (1976) 41:189
19. Chang JC, Kim YM, Duff KJ, Das TP (1976) Theor Chim Acta 41:37; Mun SK, Chang JC, Das TP (1977) Biochim Biophys Acta 490:249; Mallick MK, Mun SK, Mishra S, Chang JC, Das TP (1978) Hyperfine Interactions 4:914
20. Chang JC, Das TP (1978) Biochim Biophys Acta 502:61; Mun SK, Chang JC, Das TP (1979) J Am Chem Soc 101:5562; Mun SK, Chang JC, Das TP (1979) Proc Nat Acad Sci (USA) 76:4842
21. Mishra SL, Chang JC, Das TP (1980) J Am Chem Soc 102:2674; Mishra KC, Mishra SK, Scholes CP, Das TP (1983) J Am Chem Soc 105:7553; Mishra KC, Mishra SK, Das TP (1983) J Am Chem Soc 105:7729; Sahoo N, Das TP (1990) Hyperfine Interactions 61:1197
22. Hoffmann R (1963) J Chem Phys 39:1397
23. Jefferey PH, Thibeault JC, Hoffmann R (1975) J Am Chem Soc 97:4884
24. Roy JN, Mishra SK, Mishra KC, Das TP (1987) Hyperfine Interactions 35:961
25. Johnson CE: Ref. 11; Van Camp HL et al: Ref. 8; Scholes CP et al: Ref. 7; Mulks CF et al.: Ref. 8
26. Chang JC et al: Refs. 18–20; Mallick MK et al: Refs. 16 and 19
27. Koenig DF (1965) Acta Cryst 18:663
28. Sahoo N et al: Ref. 3; Sahoo N, Das TP (1990) J Chem Phys 93:1200; Ramani Lata K, Sahoo N, Das TP (1991) J Chem Phys 94:3715
29. Hay PJ (1977) J Chem Phys 66:4377
30. Mezey PG, Csizmadia IG (1977) Can J Chem 55:1181
31. McLean AD, Chandler GS (1980) J Chem Phys 72:5639
32. Sahoo N et al: Ref. 5; Dev BN et al: Ref. 6; Kelires PC et al: Ref. 6
33. Mulliken RS (1955) J Chem Phys 23:1833
34. Das TP (1973) Relativistic quantum mechanics of electrons, Chap 4. Harper and Row, NY
35. Mishra KC et al: Ref. 21
36. Scholes CP, Lapidot A, Mascarenhas R, Inbushi T, Isaacson RA, Feher G (1982) J Am Chem Soc 104:2724
37. Johnson CE: Ref. 11
38. Van Camp HL et al: Ref. 8; Scholes CP et al: Ref. 7
39. Kelires PC, Das TP: Ref. 6; Vander Woude F (1966) Phys Stat Sol 17:417
40. Duff KJ, Das TP (1971) Phys Rev B3:2294; Hanna SS, Heberle J, Perlow GJ, Preston RS, Vincent DM (1960) Phys Rev Letters 4:513
41. Mulks CF et al: Ref. 8
42. Bagus PS, Liu PS (1966) Phys Rev 148:79
43. Ray SN, Lee T, Das TP (1973) Phys Rev B8:5291
44. Dutta NC, Matsubara C, Pu RT (1969) Phys Rev 177:33
45. McConnell HM (1972) Proc Natl Acad Sci USA 69:335; Mun SK, Mallick MK, Mishra S, Chang JC, Das TP (1981) J Am Chem Soc 103:5024
46. Koenig SH, Brown III RD (1984) Mag Reson Med 1:478; Gore JC (1985) IEEE Eng Med Bio Mag 85:30; Bloembergen N, Purcell EM, Pound RW (1948) Phys Rev 73:678
47. Abragam A (1961) Principles of nuclear magnetism, Chap 8. Oxford Univ Press, London; Solomon I (1955) Phys Rev 99:559; Kubo R, Tomita T (1954) J Phys Soc Jpn 9:888
48. Andrew ER (1956) Nuclear magnetic resonance. Cambridge Univ Press, Cambridge; Slichter CP (1978) Principles of magnetic resonance. Springer-Verlag, Berlin; Saha AK, Das TP (1957) Nuclear induction. Saha Institute of Nuclear Physics, Calcutta

49. Wertz JE, Bolton JR (1972) Electron paramagnetic resonance. McGraw-Hill, NY; Van Camp HL, Scholes CP, Mulks CR, Caughey MS (1977) J Am Chem Soc 99:8393
50. It should be noted though that in principle, the UHF wavefunction is not strictly an eigen-function of S^2. When one uses projection operator techniques to make it an eigen-function of S^2 to obtain a PUHF wavefunction, the latter contains some many-body effects (see for instance, page 5 of Chang ES, Pu RT, Das TP (1968) Phys Rev 174:1). However, in our present calculations, it was found that the expectation value of S^2 was very close to 8.75, the value of $S(S+1)$ when $S = 5/2$. No resort to a PUHF wavefunction was therefore necessary and hence there is no many-body effect included in the present UHF calculation.
51. Lee T, Das TP (1972) Phys Rev A6:962; Rodgers JE, Lee T, Ikenberry D, Das TP (1973) Phys Rev A7:51; Rodgers JE, Das TP (1973) Phys Rev A8:3675